Combined kinetic and DFT studies on the stabilization of the pyramidal form of H_3PO_2 at the heterometal site of $[Mo_3M'S_4(H_2O)_{10}]^{4+}$ clusters (M'= Pd, Ni) †

Andrés G. Algarra,[a] María J. Fernández-Trujillo,[a] Vicent S. Safont,[b] Rita Hernández-Molina[c,*] and Manuel G. Basallote,[a,*]

[a] Departamento de Ciencia de los Materiales e Ingeniería Metalúrgica, Facultad de Ciencias, Universidad de Cádiz, Avd. República Saharahui, s/n, Puerto Real, 11510 Cádiz, Spain. [b] Departament de Química Física i Analítica, Universitat Jaume I, Avda. Sos Baynat s/n, 12071 Castelló, Spain. [c] Departamento de Química Inorgánica, Facultad de Farmacia, Universiad de La Laguna, 38200 La Laguna, Tenerife, Spain.

E-mail: manuel.basallote@uca.es; rrhernan@ull.es.

† Electronic supplementary information (ESI) available: Cartesian coordinates geometries and energies for the different species optimized by DFT procedures.

Summary

Kinetic and DFT studies have been carried out on the reaction of the $[Mo_3M'S_4(H_2O)_{10}]^{4+}$ clusters (M'= Pd, Ni) with H_3PO_2 to form the $[Mo_3M'(pyr\text{-}H_3PO_2)S_4(H_2O)_9]^{4+}$ complexes, in which the rare pyramidal form of H_3PO_2 is stabilized by coordination to the M' site of the clusters. The reaction proceeds with biphasic kinetics, both steps showing a first order dependence with respect to H_3PO_2. These results are interpreted in terms of a mechanism that involves an initial substitution step in which one tetrahedral H_3PO_2 molecule coordinates to M' through the oxygen atom of the P=O bond, followed by a second step that consists in tautomerization of coordinated H_3PO_2 assisted by a second H_3PO_2 molecule. DFT studies have been carried out to obtain information on the details of both kinetic steps, the major finding being that the role of the additional H_3PO_2 molecule in the second step consists in catalysing a hydrogen shift from phosphorus to oxygen in O-coordinated H_3PO_2, which is made possible by its capability of accepting a proton from P-H to form $H_4PO_2^+$ and then transfer it to the oxygen. DFT studies have been also carried out on the reaction at the Mo centres to understand the reasons that make these metal centres ineffective for promoting tautomerization.

Introduction

The importance of phosphorus in transition metal chemistry is widely recognized, mainly because the use of phosphine ligands has allowed to modulate steric and electronic properties of the resulting metal complexes.[1, 2] Nowadays, the search for appropriate ligand sets that effectively control the reactivity and stability of metal complexes continues to play an essential role in inorganic and organometallic chemistry. However, while there are many studies involving the use of phosphine ligands, little is known about the coordination chemistry of other stable forms of phosphorus as its oxoacids. In this sense, important advances have been done during the last decade with respect to the properties of phosphorus acids in the lower oxidation states acting as ligands. As an example, Jagirdar et al. have shown that the 16 electron complex $[Ru(P(OH)_3)(dppe)_2][OTf]_2$ (dppe= $Ph_2PCH_2CH_2PPh_2$), which possess a $P(OH)_3$ pyramidal group, activates the H-H (in H_2(g)), the Si-H (in silanes) and the B-H bonds (in borane-Lewis base adducts).[3, 4]

Hypophosphorous acid (systematic name phosphinic acid) can adopt two different tautomeric structures: the tetrahedral form (*tet*) [$H_2PO(OH)$] is the most stable one and contains two hydrogen atoms directly bound to the phosphorus, whereas the pyramidal form (*pyr*) [$HP(OH)_2$] only has one P-H bond and there is a lone pair of electrons over the phosphorus atom (see Scheme 1).[5, 6] For a long time it was impossible to isolate or observe directly this *pyr* form of the acid, though its presence in equilibrium with the *tet* tautomer was repeatedly postulated from kinetics studies,[7-9] and it was estimated that the *pyr*/*tet* ratio in aqueous solutions does not exceed 10^{-12}.[10] Nowadays it is known that the unstable *pyr*-H_3PO_2 tautomer can be stabilized via coordination to a soft metal center and, as a matter of fact, there are several well-characterized metal complexes containing the *pyr* forms of H_3PO_2 and related acids in low oxidation states.[3, 11-17] At this point it is important to note the relevant role that $M_3M'Q_4$ cuboidal clusters (M= Mo, W; Q= S, Se; M'= Ni, Pd...) have played in this field.[12-17]

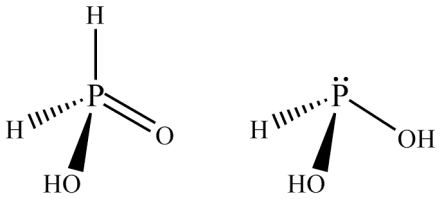

tet-H_3PO_2 *pyr*-H_3PO_2

Scheme 1

Given our interest in the mechanistic aspects of reactions of M_3Q_4 and $M_3M'Q_4$ cuboidal clusters, we decided to carry out an experimental and theoretical study of the reaction shown in eq 1, and some results have been published in a previous communication.[18] As shown in eq 1, addition of an excess of H_3PO_2 to the $[Mo_3PdS_4(H_2O)_{10}]^{4+}$ (**1**) and $[Mo_3NiS_4(H_2O)_{10}]^{4+}$ (**1**Ni) clusters leads to the formation of $[Mo_3Pd(pyr\text{-}H_3PO_2)S_4(H_2O)_9]^{4+}$ (**2**) and $[Mo_3Ni(pyr\text{-}H_3PO_2)S_4(H_2O)_9]^{4+}$ (**2**Ni), respectively.

$$[Mo_3M'S_4(H_2O)_{10}]^{4+} + H_3PO_2 \rightarrow [Mo_3M'(pyr\text{-}H_3PO_2)S_4(H_2O)_9]^{4+} \quad ; M'= Pd, Ni \quad (1)$$

Kinetic studies revealed that this process takes place in two consecutive steps, and it was proposed that the first one consists in O-coordination of *tet*-H_3PO_2 whereas the second one involves isomerization and P-coordination of the acid (Scheme 2). While the first step is a simple substitution, the second one involves different processes with participation of an external second *tet*-H_3PO_2 molecule, so that the previous communication focused on the mechanism of this second step. In the present paper we discuss in more detail the previous

findings and pay attention to other important aspects of this kind of reactions by means of DFT calculations, in particular the reasons that lead to the absence of reaction over the Mo centres and the characteristics of the water substitution, i.e. the first step of the proposed mechanism. All the theoretical work has been carried out over the Pd cluster **1**, although the small kinetic differences between both clusters make reasonable to extrapolate the conclusions to **1**Ni.

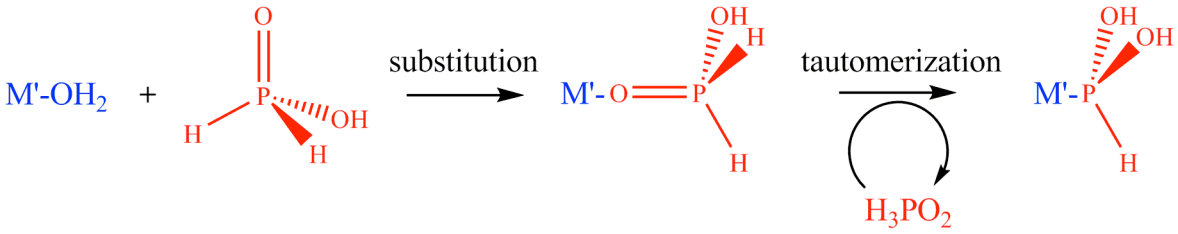

Scheme 2. Mechanism proposed for the reaction of H_3PO_2 with clusters **1** and **1Ni**. For simplicity only the M' site of the cluster is shown.

Results and Discussion

Kinetics of reaction of $[Mo_3M'S_4(H_2O)_{10}]^{4+}$ clusters (M'= Pd, Ni) with H_3PO_2

Stopped flow experiments reveal that the reaction of **1** or **1**Ni with an excess of H_3PO_2 (eq. 1) in aqueous solution (25.0ºC, 2.0 mol dm^{-3} Hpts/Lipts, pts^-= p-toluenesulfonate) occurs with biphasic kinetics, thus showing the existence of a detectable reaction intermediate. Surprisingly, the rate constants for both steps show a first order dependence with respect to *tet*-H_3PO_2, which indicates that stabilization of a single *pyr*-H_3PO_2 requires the participation of two *tet*-H_3PO_2 molecules, one in each step. The values of the second order rate constants for the Pd cluster (**1**) are k_1= (12.5±0.3)×10^{-2} $mol^{-1}dm^3s^{-1}$ and k_2= (2.6±0.1)×10^{-2} $mol^{-1}dm^3s^{-1}$, and they do not change with $[H^+]$ (0.5-2.0 mol dm^{-3} range), which suggests that the only species that contribute significantly to the reaction rate are **1** and H_3PO_2. Actually, the absence within that pH range of hydroxo complexes derived from **1** have been confirmed previously,[19] but the pK_a of H_3PO_2 is close to 1 and significant amounts of $H_2PO_2^-$ can exist in the solutions used for the kinetic studies. However, participation of this anion in any of both kinetic steps can be reasonably ruled out because it would lead to a significant increase in the rate constants when $[H^+]$ decreases. The related Ni complex (**1**Ni) shows similar kinetics, although the second step occurs under conditions of reversible equilibrium, in agreement with the reported lower reactivity of **1**Ni.[12] The values of the rate constants for **1**Ni are k_1= (2.38±0.05)×10^{-2} $mol^{-1}dm^3s^{-1}$, k_{2forw}=

$(1.00\pm0.06)\times10^{-4}$ $mol^{-1}dm^3s^{-1}$ and k_{2rev}= $(1.76\pm0.05)\times10^{-5}$ s^{-1}. Figure 1 shows the kinetic data for the reaction of cluster **1**Ni with an excess of H_3PO_2 and the electronic spectra of the species involved in this reaction as calculated from the kinetic data are included in Figure 2. It is interesting to note that the electronic spectra of both intermediates, **I** and **I**Ni resembles that of the starting complexes **1** and **1**Ni respectively, which suggests that the coordination environments around the metal centres do not change significantly in the first kinetic step, thus making reasonable the assumption that this step is a simple substitution leading to intermediates with O-coordinated H_3PO_2.

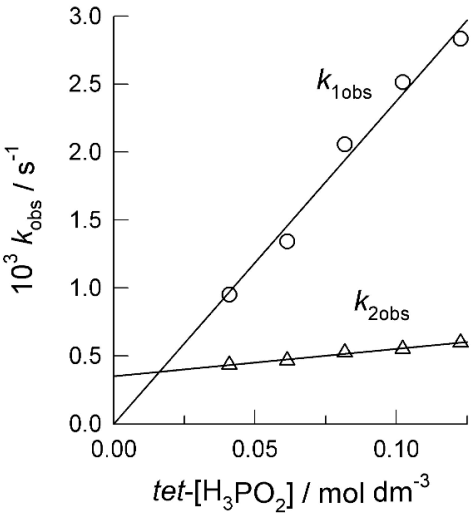

Figure 1. Plots of the dependence with the *tet*-H_3PO_2 concentration of the observed rate constants for the reaction of cluster **1**Ni with *tet*-H_3PO_2. The circles and triangles correspond to the first and second steps, respectively.

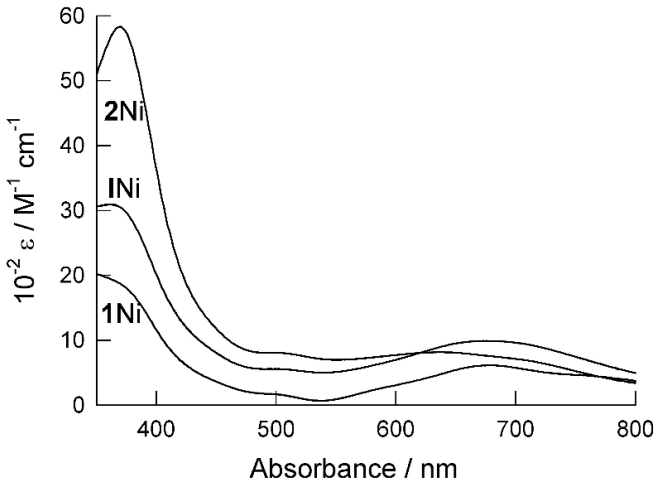

Figure 2. Electronic spectra calculated from kinetic data for the species involved in the reaction of **1**Ni with *tet*-H_3PO_2.

Monitoring the reaction of the palladium complex **1** with $^{31}P\{^1H\}$ NMR confirmed that the only reaction product is **2**, characterized by a singlet at 122.0 ppm that converts to a doublet ($^1J_{P,H}$= 414 Hz) in the proton-coupled phosphorus spectrum. The appearance of a single signal for the reaction product indicates that tautomerization only occurs at Pd, i.e. the Mo centers are ineffective for this process, which is in agreement with the lower lability of the Mo centres in **1**[19] and with all reported crystal structures for these compounds.[13-17, 19, 20] Unfortunately, no NMR signal could be observed for the intermediate, probably because of rapid exchange between coordinated and free H_3PO_2.

DFT study of the reaction over the Pd site in $[Mo_3PdS_4(H_2O)_{10}]^{4+}$ (1)

As the kinetic results indicate the existence of two separate steps for the reaction in eq 1 and the similarity of the spectra calculated for the reaction intermediate with respect to those of the starting complexes suggests that the coordination environment about the metal centres does not change in the first step, the mechanism in Scheme 2 continues being the most reasonable proposal. In this section DFT results for both steps are presented, starting with the initial substitution. All calculations have been carried out with cluster **1**, although no important changes must be reasonably expected for the Ni cluster.

First step: Substitution at the Pd centre

As the first step involves a simple substitution of coordinated water, the process can be assumed to occur through the classical Eigen-Wilkins mechanism, in which complex formation starts with a rapid preequilibrium of formation of an outer-sphere complex followed by rate-determining substitution of water by the entering ligand. The structural and energy changes for this mechanism have been modelled by DFT procedures, and the optimized geometries of the different species involved are shown in Figure 3**,** while Figure 4 shows an energy profile of the reaction over this centre. Although some structures show the existence of an intramolecular hydrogen bond, additional calculations showed that it does not play a significant role in the tautomerization process. According to the DFT results, substitution of the water molecule coordinated to palladium starts with the formation of an outer sphere complex between **1** and *tet*-H_3PO_2 (*osc*-1), which is stabilized by 1.7 kcal/mol

with respect to the separated reagents. In *osc*-1, the *tet*-H_3PO_2 molecule is interacting both with the Pd-coordinated water and with one of the coordinated waters of the nearest Mo centre. Obviously, there are alternative structures for the outer sphere complex, and actually a more stable one will be shown below when discussing the reaction at the Mo sites, but it is this one from which we have been able to obtain a transition state, TS(1toI), that connects it with the product of substitution at the Pd site, i.e. intermediate **I**. It is also interesting to note that the proximity of the entering H_3PO_2 to both types of metal centres in the structure of this outer-sphere complex makes it the starting point for substitution not only at Pd but also at Mo, as will be shown below.

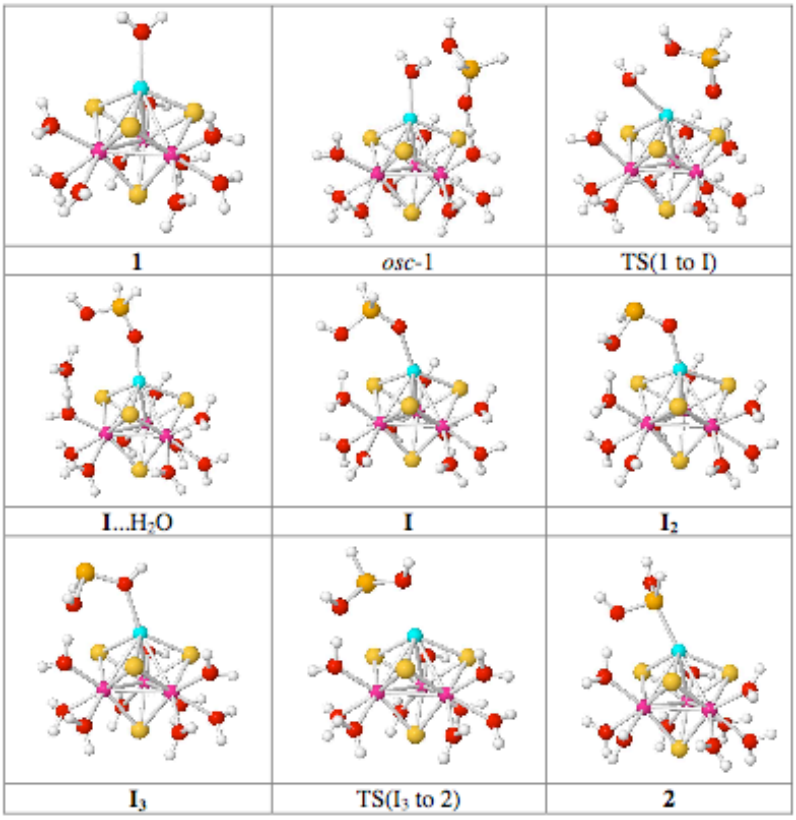

Figure 3. Optimized geometries for the species involved in the reaction over the Pd centres.

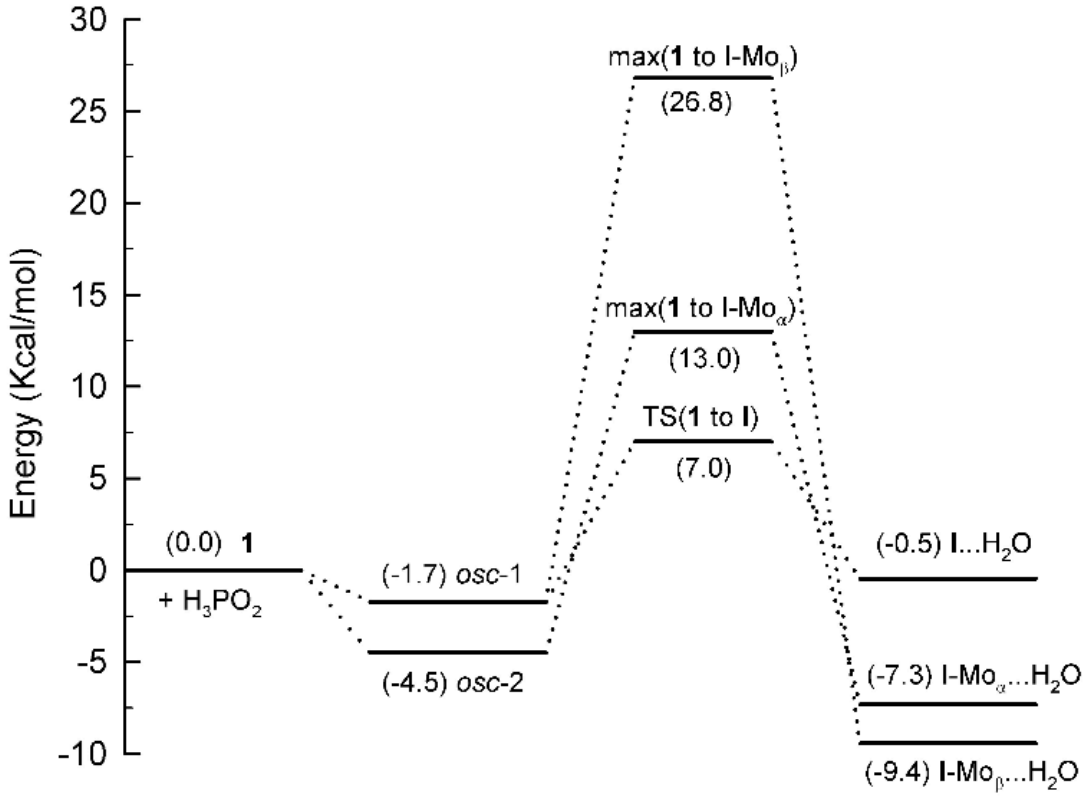

Figure 4. Energy profile for the first observable step both at the Pd site and the *c* and *d* Mo sites.

TS(1toI) is 7.0 kcal/mol higher in energy than the separate reagents, so that the activation barrier for substitution is calculated to be 8.7 kcal/mol. The Pd-O distances in TS(1toI) are 2.472 Å for the leaving water molecule and 3.128 Å for the closest oxygen of the entering H_3PO_2, so that there is a significant approach of the entering ligand before the leaving water separates from the metal centre. The substitution product is intermediate **I...H_2O**, which contains a *tet*-H_3PO_2 O-coordinated to the palladium center and a water molecule hydrogen-bonded both to the coordinated H_3PO_2 and to one Mo-coordinated water molecule. As **I...H_2O** is 0.5 kcal/mol lower in energy than the separated reagents, the whole substitution process can be practically considered as a thermoneutral reaction. In a previous experimental study of substitution reactions in **1** using a variety of entering ligands (Cl^-, Br^-, SCN^-, CO, TPA, $TPPTS^{3-}$),[19] it was found that substitutions of the water coordinated at the Pd centre by these ligands are too fast to be measured by stopped-flow techniques, and a predominantly dissociative I_d mechanism was tentatively proposed because all of these substitutions were assumed to occur with similar rate constants for the different ligands. However, when those results are taken together with those in the present work for the reaction with H_3PO_2, an

important effect of the entering ligand on the kinetics of substitution is evident. From this comparison and from the structure derived for the transition state in the DFT studies, we consider that substitutions at the Pd site can be better designed as occurring through a predominantly associative interchange mechanism.

Second step: Tautomerization of the Pd-coordinated tet-H_3PO_2.

As stated above, the second resolved kinetic step in the reaction of **1** or **1**Ni with an excess of H_3PO_2 shows in both cases a first order dependence with respect to the concentration of H_3PO_2. This rate law is unexpected for a process that formally involves coordination and tautomerization of a single H_3PO_2 molecule (eq. 1). This kinetic finding cannot be explained with simple mechanisms involving tautomerization of free H_3PO_2 followed by coordination of the resulting *pyr* form. Thus, a fast pre-equilibrium between both tautomeric forms followed by rate-determinimg reaction of *pyr*-H_3PO_2 with **1** or **1**Ni would lead to the observation of a single kinetic step. On the other hand, slow tautomerization of H_3PO_2 followed by coordination of the *pyr* form could result in biphasic kinetics but the rate of the first step should be independent of the nature of the cluster. Alternative mechanisms involving coordination at the Mo centres will be discussed below, although at this time it must be pointed out that substitutions at these centres are known to be significantly slower than at Pd.[19] In contrast, it has been demonstrated that inter-conversion between the *tet* and *pyr* forms of compounds with the functional group >P(O)H can take place by either an unimolecular or a bimolecular mechanism, the bimolecular mechanism being favoured because the activation barrier is significantly lower in all cases.[21] Thus, both the experimental finding and the DFT precedents lead to the inclusion of a second *tet*-H_3PO_2 molecule in the calculations, and the results so obtained proved to be very useful for understanding the way in which it could assist tautomerization of the previously coordinated one.

The starting point of the DFT calculations for this second step is intermediate **I** formed in the previous step. Although calculations described above lead to a species (**I...H_2O**) containing a hydrogen bonded water molecule, for simplicity the latter has been omitted in the calculations for the second kinetic step. Although it is evident that this intermediate, as well as other species described in this section, will surely form a network of hydrogen bonds with water molecules in the second coordination sphere and that those interactions will surely lead to changes in the values of the energy derived for the different processes, the major features of the mechanism could be obtained from calculations without considering any additional water molecule.

The product formed in the second kinetic step is complex $[Mo_3Pd(pyr\text{-}H_3PO_2)S_4(H_2O)_9]^{4+}$ (**2**), that contains a *pyr*-H_3PO_2 molecule P-coordinated to the palladium centre. In agreement with the experimental observations, DFT calculations indicate that **2** is 13.8 kcal/mol more stable than **I**, so that tautomerization of coordinated H_3PO_2 is thermodynamically favoured. The conversion of **I** to **2** is proposed to occur through the mechanism depicted in Figure 5, and the geometries of all the species involved are included in Figure 3. Tautomerization starts with a proton transfer from one of the P-H bonds to an external *tet*-H_3PO_2 molecule, thus yielding to a complex ($\mathbf{I}_2$) that contains O-coordinated *pyr*-H_3PO_2. This proton transfer implies the formation of $H_4PO_2^+$, which is made possible by the capability of H_3PO_2 to act as a base, and actually other reactions of H_3PO_2, as H/D exchange and oxidations with several reagents, have been also proposed to take place with formation of $H_4PO_2^+$.[7-9] Proton abstraction from a P-H bond has been also found to be relevant in the mechanism of the Atherton-Todd reaction of oxidation of dialkyl phosphonates with chlorocarbons.[22] The calculations show that conversion of **I** to $\mathbf{I}_2$ has a moderate energy cost (22.4 kcal/mol) and it takes place without any additional activation barrier, as revealed by scan calculations (see Figure 6). The energy profile in Figure 7 (black lines) for the overall tautomerization process indicates that this is the most energy-demanding step, so that it is expected to be the rate determining step in the second step observed in the stopped-flow experiments, i.e. the tautomerization process.

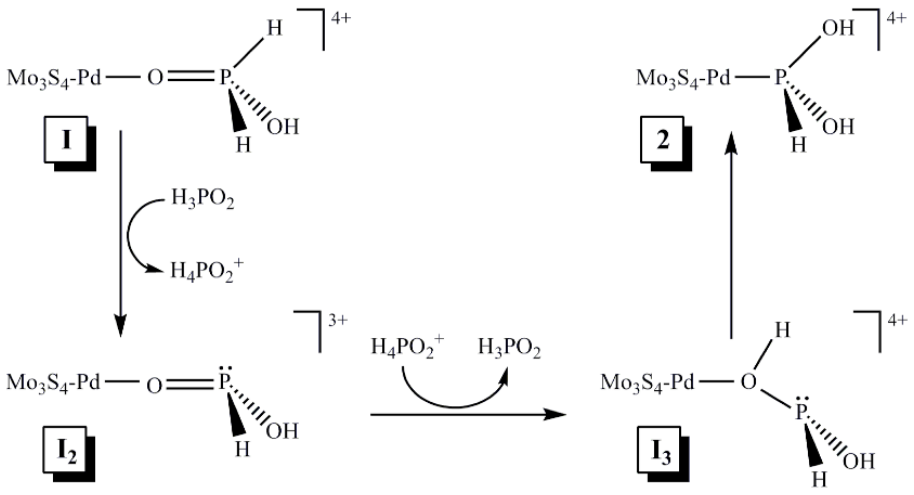

Figure 5. Mechanism proposed for tautomerization of coordinated H_3PO_2 at the Pd site of cluster **1** assisted by a second H_3PO_2 molecule.

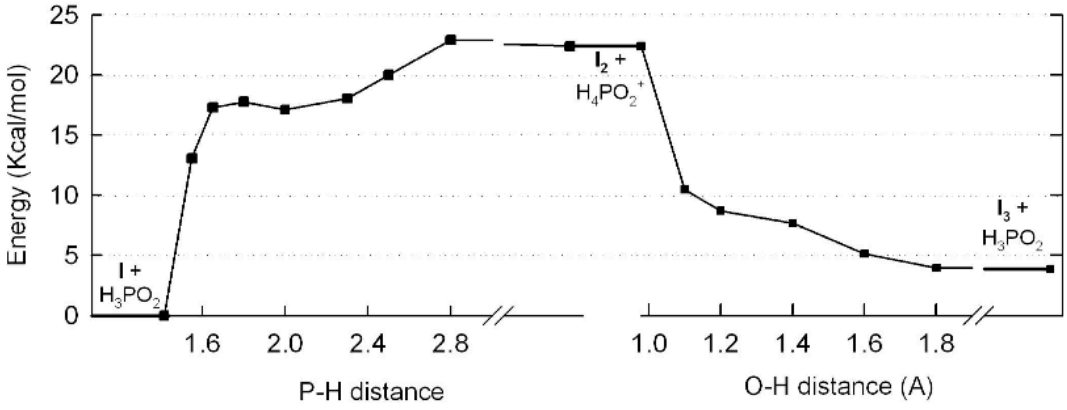

Figure 6. Potential energy curves for the **I** → **I**$_2$ (left) and **I**$_2$ → **I**$_3$ (right) processes taking the P-H and O-H distances as reaction coordinates, respectively. In both cases the distances refer to those with hydrogen atom transferred in the process.

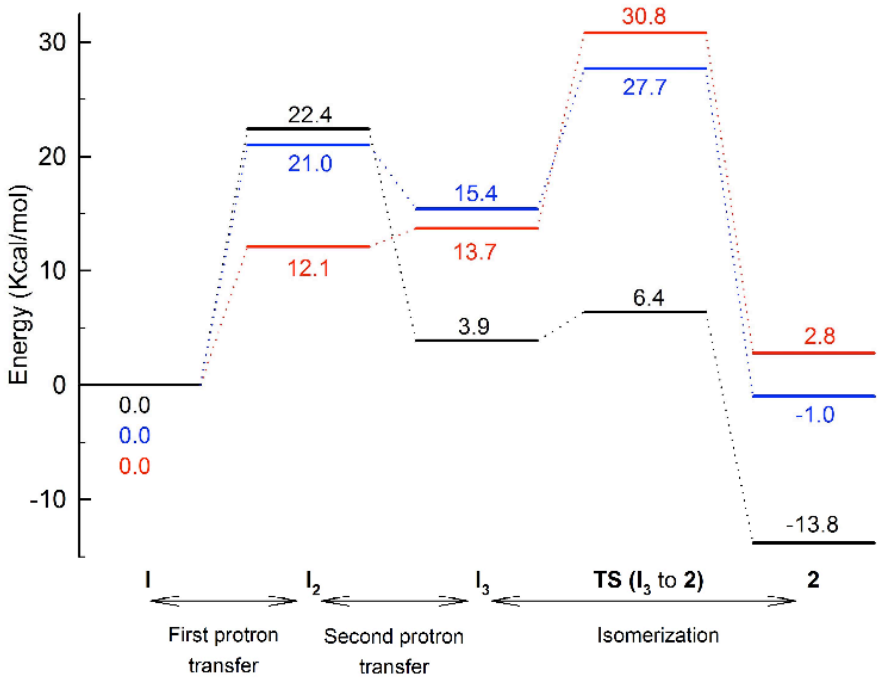

Figure 7. Energy profile for tautomerization of coordinated H_3PO_2 both at the Pd site (black) and the α (red) and β (blue) Mo sites. Note that the zero values of the energy have been taken

in all cases as those of the corresponding intermediates formed in the first step (I, I-Mo_α and I-Mo_β) and that the energies of TS(I_3-Mo_α to 2-Mo_α) and TS(I_3-Mo_β to 2-Mo_β) were estimated from scan calculations.

The reaction continues with protonation of $\mathbf{I}_2$ by $H_4PO_2^+$, which in this case acts as an acid. The transferred proton remains bonded to the oxygen atom coordinated to the palladium centre, thus leading to an intermediate $\mathbf{I}_3$ that contains an O-coordinated *pyr*-H_3PO_2. This process is favoured by 18.5 kcal/mol and it also occurs without activation barrier, as revealed by scan calculations whose results are also shown in Figure 6. The net effect of the two proton transfers is a hydrogen shift from phosphorus to oxygen, the second *tet*-H_3PO_2 molecule acting as a catalyst for the process because of its capability to act as a base and as an acid. This provides a reaction pathway much more effective than the alternative one involving direct conversion of **I** to $\mathbf{I}_3$ in absence of a second *tet*-H_3PO_2 molecule, for which a transition state with a high activation barrier (63.2 kcal/mol) could be also located by DFT procedures. The structure of this alternative transition state is included in the Supporting Information and it is quite similar to that found for isomerization of free *tet*-H_3PO_2, and actually the activation barrier found in the latter case (65.3 kcal/mol) [21] is also similar.

Once intermediate $\mathbf{I}_3$ is formed, reaction is completed with isomerization of $\mathbf{I}_3$ to **2**, where the starting O-coordinated *pyr*-H_3PO_2 ends up P-coordinated. Isomerization occurs through a transition state with a very low activation barrier of only 2.5 kcal/mol, so that it does not represent any additional energy cost for the overall process occurring in the second resolved kinetic step. As shown in Figure 7, the final product **2** is 17.7 kcal/mol more stable than $\mathbf{I}_3$ and therefore 14.3 kcal/mol more stable than the starting reagents, thus showing that the stabilization of *pyr*-H_3PO_2 at the Pd site of cluster **1** is thermodynamically favoured. The energy profiles found in the DFT calculations for both steps (see Figures 4 and 7) are also in agreement with the experimental observation of two resolved kinetic steps, the second one being slower than the first.

DFT studies exploring the possibility of H_3PO_2 tautomerization at Mo centres of $[Mo_3PdS_4(H_2O)_{10}]^{4+}$ (1)

Once explored the reaction pathway that leads to the final product **2**, attempts were made to obtain DFT information about the reasons that make the molybdenum centres ineffective for the stabilisation of *pyr*-H_3PO_2. Actually, there are several experimental findings that indicate the lower reactivity of the Mo centres in $Mo_3M'S_4$ (M´= Pd, Ni) clusters in comparison with

the heterometallic M' sites. In fact, neither the ^{31}P-NMR data obtained during the monitoring of the reaction of **1** with H_3PO_2 nor the crystal structures of the cuboidal clusters which contain phosphorus acids in low oxidation states show any evidence of coordination over the molybdenum centres. In addition, the lower lability of these centres with respect to the M' heterometal has been previously described by the group of Sykes in their comprehensive studies of the kinetic properties of cuboidal $M_3M'Q_4$ clusters.[23, 24] These works also highlighted the existence of two different kinds of H_2O molecules coordinated to M in these clusters, those which are below the plane defined by the three M centres and those which are above them, which according to Sykes nomenclature are designated, respectively, as α and β ($M_3M'Q_4$ clusters) or *c* and *d* (M_3Q_4 clusters) (see Scheme 3).[19]). It has been demonstrated that waters at the *c* position are ca. 10^5 times more labile than *d* in the substitution reactions of the incomplete analogous $[Mo_3S_4(H_2O)_9]^{4+}$ cluster.[24] With the aim to take into account these precedents, the theoretical study of the reaction of H_3PO_2 at one of the Mo sites has been carried out considering that the process starts with substitution of each one of the two different water molecules coordinated to Mo that **1** has.

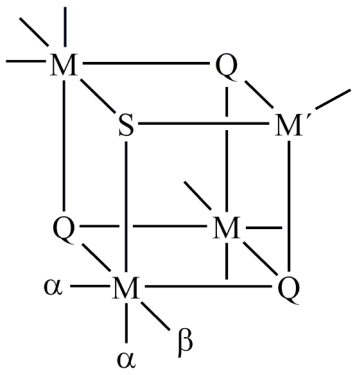

Scheme 3. Structure of cuboidal $M_3M'Q_4$ clusters showing the different types of water molecules coordinated at each metal center.

First step: Substitution at the Mo centre

According to the same mechanism proposed for the reaction at the Pd centre, substitution of each one of the two different types of Mo-coordinated water molecules would start with formation of an outer sphere complex that evolves to an intermediate with O-coordinated *tet*-H_3PO_2. These processes have been examined by DFT procedures and the geometries of all the

species involved are presented in Figure 8. Unfortunately, in contrast to substitution at Pd, the existence of several hydrogen bonds between Mo-coordinated water molecules themselves or with the entering acid prevented us to locate the transition states for substitution of the two kinds of water molecules (α and β). For this reason, relaxed scan calculations were carried out by taking as reaction coordinate the distance between one of the Mo centres and the O atom of the P=O bond in *tet*-H_3PO_2, this coordinate being changed from the distance in the outer sphere complexes to that in the intermediates with O-coordinated *tet*-H_3PO_2, i.e. **I**-Mo_α and **I**-Mo_β (see Figure 9).

Substitution at one β water molecule starts with the formation of the same outer sphere complex as the one formed during the substitution of the palladium coordinated water, i.e. intermediate *osc*-1, which is only 1.7 kcal/mol more stable than the separate reagents. Scan calculations indicate the existence of an energy barrier for substitution of 26.8 kcal/mol with respect to *osc*-1, which is as expected significantly larger than the barrier for reaction at the Pd site. The product formed in this reaction pathway is an intermediate that contains a *tet*-H_3PO_2 molecule O-coordinated to the β site and a hydrogen-bonded water molecule, **I**-Mo_β...H_2O. This product is 9.4 kcal/mol more stable than the separated reagents, so its formation constitutes an exotermic reaction.

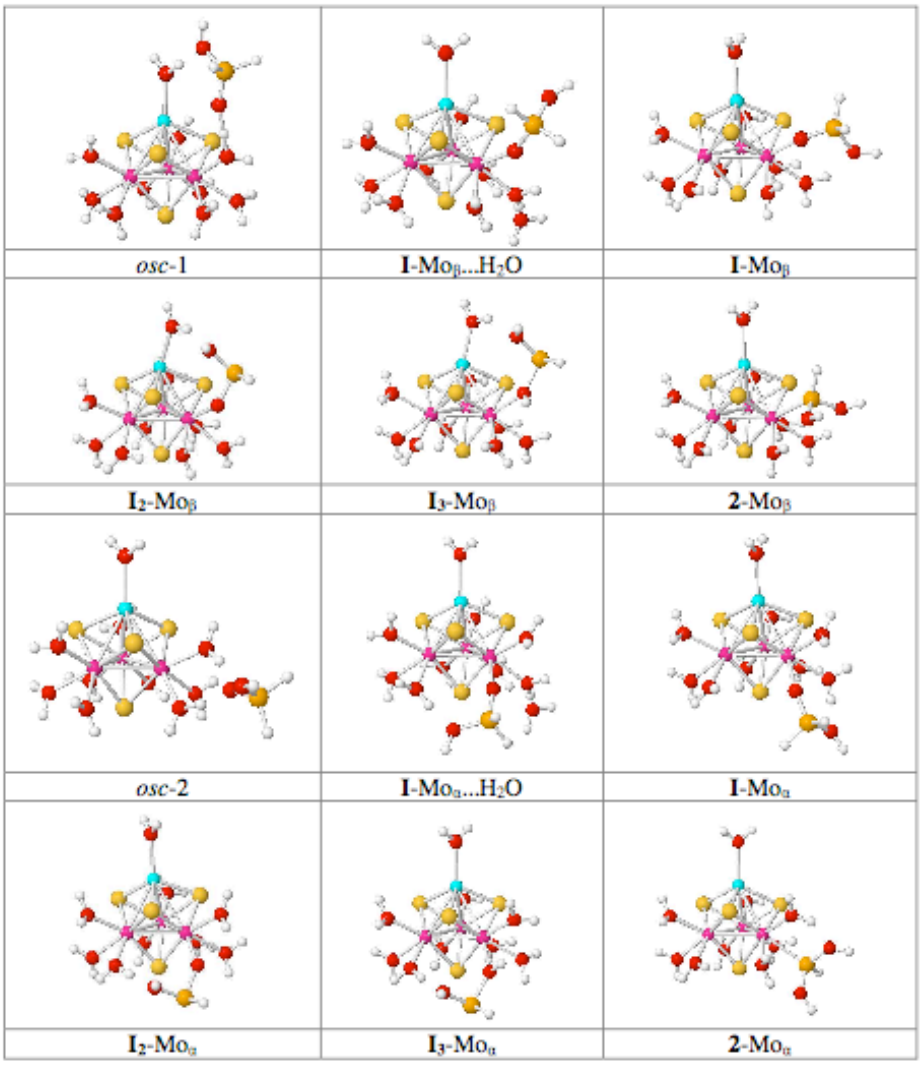

Figure 8. Optimized geometries for the species involved in the reaction over the α and β Mo sites of cluster **1**.

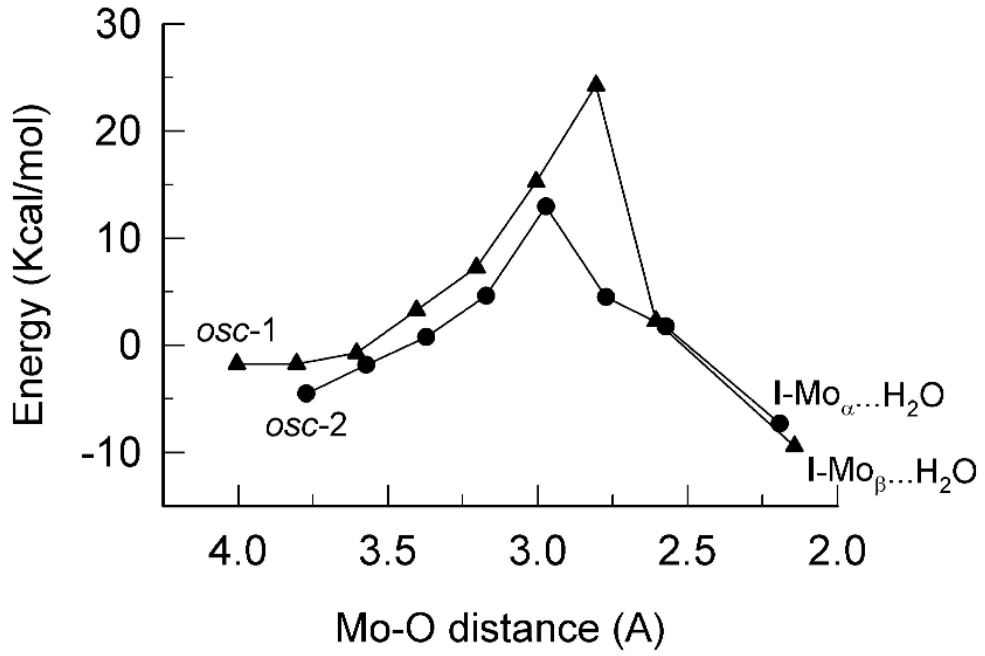

Figure 9. Potential energy curves for the *osc*-1 → **I**-Mo$_\beta$ and *osc*-2 → **I**-Mo$_\alpha$ processes taking the Mo-O distance as the reaction coordinate. The circles represent the reaction at the α site while triangles represent the reaction at the β site.

On the other hand, substitution of one of the α water molecules starts with formation of a different outer sphere complex (*osc*-2) which is 4.5 kcal/mol more stable than the separated reagents. The higher stability of this outer sphere complex with respect to *osc*-1 is caused by the interaction of the P=O group with two different water molecules coordinated to the same molybdenum center. The substitution product (**I**-Mo$_\alpha$...H$_2$O), which also contains an O-coordinated *tet*-H_3PO_2 and a hydrogen-bonded water molecule, is 7.3 kcal/mol more stable than the separated reagents, and scan calculations indicate that its formation takes place through an energy barrier of 17.5 kcal/mol with respect to *osc*-2. Therefore, these results indicate that if the substitution would take place at one molybdenum centre, it would occur at a α site for kinetic reasons. These results are in good agreement with the different lability observed for the α and β water molecules in similar cuboidal clusters,[25] and can also explain the fact that reaction only takes place over the palladium centre. Thus, the comparison in Figure 4 of the reaction pathways in the substitution of H_2O/Pd, H_2O/Mo$_\alpha$ and H_2O/Mo$_\beta$ molecules clearly shows the higher lability of the Pd centre, although substitution at the Mo centres is more favoured from the thermodynamic point of view and it should be expected to

occur in a longer timescale. It is important to note that these calculations provide for the first time DFT support for the different lability of coordinated water molecules in cuboidal clusters, and more work related to it is currently in progress.

Second step: Tautomerization of the Mo-coordinated tet-H3PO2 acid.

Once established by DFT procedures that it is possible to achieve the species **I**-Mo_{α} and **I**-Mo_{β} with a non-prohibitive energy cost, the possibility of tautomerization of coordinated H_3PO_2 in both species was examined assuming that the processes take place according to the same mechanism as proposed for the reaction at the palladium center. Therefore, tautomerization would start with two consecutive proton transfers between **I**-$Mo_{\alpha,\beta}$ and a second *tet*-H_3PO_2 molecule, thus leading to $\mathbf{I}_2$-$Mo_{\alpha,\beta}$ and subsequently to $\mathbf{I}_3$-$Mo_{\alpha,\beta}$, which finally converts to the hypothetical reaction products **2**-$Mo_{\alpha,\beta}$. The geometries obtained for all of these species are also given in Figure 8, and the energy profiles for tautomerization at the three sites of the cluster are compared in Figure 7. The major conclusion from these results is that the H_3PO_2-assisted tautomerization of O-coordinated H_3PO_2 is thermodynamically favoured at the Pd site but it is almost thermoneutral at the Mo centres, in such a way that there is a difference of 12.8-15.6 kcal mol^{-1} favouring reaction at the Pd site, in agreement with the experimental observations. Nevertheless, these energy values must be taken again with care for the reasons given above.

The energy cost associated to the formation of intermediates $\mathbf{I}_2$ and $\mathbf{I}_2$-Mo_{β} is very similar and, what is more surprising, formation of $\mathbf{I}_2$-Mo_{α} is even more favoured than the corresponding process at the Pd site. From this result and the lower barrier to substitution at the α sites with respect to β, it can be concluded that reaction at the α site continues being the most plausible site of reaction at the Mo centre. Nevertheless, there is an important difference between the thermodynamic parameters for the second proton transfer at the Mo_{α} and Pd sites that makes the Mo_{α} site less reactive: while formation of $\mathbf{I}_3$ from $\mathbf{I_2}$ constitutes an exothermic process, formation of $\mathbf{I}_3$-Mo_{α} is endothermic. Moreover, the energy profiles in Figure 7 indicate that the relative stabilities of the different $\mathbf{I}_3$ intermediates clearly favour reaction at the Pd site, mainly because of the higher stabilisation achieved in the second proton transfer process involving the second H_3PO_2 molecule.

The hypothetical tautomerization process at the Mo sites would finish with the conversion of the O-coordinated species $\mathbf{I}_3$-$Mo_{\alpha,\beta}$ to the P-coordinated **2**-$Mo_{\alpha,\beta}$. As in the case of the initial

substitution process, the many possibilities of hydrogen bonding prevented us to locate the transition state for the isomerization at **I**$_3$-Mo$_{\alpha,\beta}$. However, scans calculations using the Mo-P distance as the reaction coordinate provided approximate values for the energy costs associated to these isomerizations, which are 17.1 and 12.3 kcal/mol for the α and β sites respectively (see Figure 10). These values make the overall energy barrier for reaction at Mo close to 30 kcal mol^{-1} from **I**, significantly higher than that obtained for isomerization at Pd. Transition states for the direct conversion of **I**-Mo$_{\alpha,\beta}$ to **I**$_3$-Mo$_{\alpha,\beta}$ (named TS(I to I$_3$)-Mo$_{\alpha,\beta}$) in the absence of a second H_3PO_2 molecule have been also located but they are also very high in energy (66.3 and 66.2 Kcal/mol respectively) and uncompetitive with the catalyzed process As a whole, the DFT results in the present section indicate that the stabilisation of *pyr*-H_3PO_2 at the metal sites of cluster **1** is clearly favoured at Pd with respect to Mo both from the thermodynamic and the kinetic points of view, although a significant decrease of the activation barrier with respect to tautomerization of free H_3PO_2 is derived also for the Mo sites. Moreover, as the energy cost associated to the transformation of O-coordinated **I**$_3$-Mo$_{\alpha,\beta}$ to the P-coordinated **2**-Mo$_{\alpha,\beta}$ isomers is very small, the possibility of tautomerization at the Mo sites cannot be excluded by using different experimental conditions or by changing the nature of the cluster, a possibility that is being currently examined.

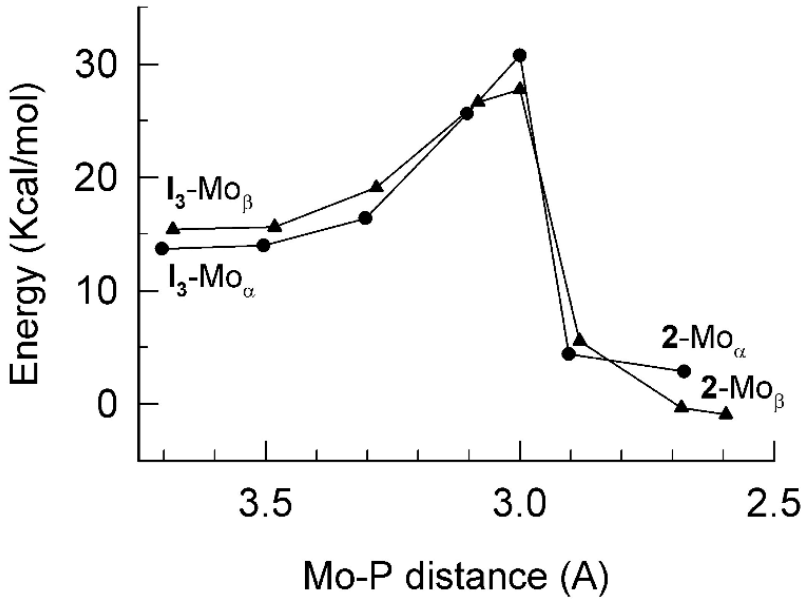

Figure 10. Potential energy curves for the **I**$_3$-Mo$_{\alpha,\beta}$ → **2**-Mo$_{\alpha,\beta}$ processes taking the Mo-P distance as the reaction coordinate. The circles represent the reaction at the α site while triangles represent the reaction at the β site.

Conclusion

The experimental and theoretical results in the present paper clearly support the mechanistic proposal for the stabilization of the unstable pyramidal form of H_3PO_2 made in a previous communication, in which the process is proposed to occur through initial O-coordination of *tet*-H_3PO_2 followed by a tautomerization step assisted by a second H_3PO_2 molecule.[18] Of particular relevance is the catalytic role played by the second H_3PO_2 molecule, which facilitates the isomerization of the previously coordinated one by allowing two consecutive proton transfer processes with the transient formation of $H_4PO_2^+$. This process allows a mechanistic pathway that reduces significantly (to ca. 20 kcal mol^{-1}) the energy barrier for tautomerization of O-coordinated *tet*-H_3PO_2 with respect to the value in free H_3PO_2 (ca. 60 kcal mol^{-1}).

It is also interesting to note that the comparative study of the process at the Pd and Mo sites of cluster **1** reveals that despite the lower stabilization achieved and the higher activation barrier, tautomerization at the Mo centres is still more favored than in free H_3PO_2. Thus, it appears that coordination at a transition metal centre activates this molecule towards the geometric changes required for tautomerization. This fact and the experimental isolation of complexes containing the pyramidal forms of H_3PO_2 and the related H_3PO_3 coordinated to transition metal complexes of a nature very different from that of the present clusters strongly suggest the possibility of developing a rich coordination chemistry based on these low-valent phosphorus ligands. The large success of phosphine complexes makes this field a tempting research field for the next future.

Experimental

Synthesis of the clusters

The green starting trinuclear cluster $[Mo_3S_4(H_2O)_9]^{4+}$ cluster was prepared according to published procedures [26, 27] and purified by Dowex-50W-X2 cation exchange chromatography. The cluster was obtained in 2M HCl aqueous solution at concentrations close to 0.01 M (UV-vis band positions λ/nm (ε/$M^{-1}cm^{-1}$): 370(4995), 616(326)).

The blue $[Mo_3(PdCl)S_4(H_2O)_9]^{3+}$ complex was prepared according to the published procedure[19, 28] by reacting Pd black with $[Mo_3S_4(H_2O)_9]^{4+}$. (UV- Vis peak positions λ/nm

($\varepsilon/M^{-1}cm^{-1}$) (450(1013) and 580(1382)). Although this complex crystallises as an edge-linked double cube[4] from concentrated solutions of Hpts, its elution behaviour indicates that in solution it exists as a single cube. When eluted with HCl, the cube has 3+ charge, consistent with Cl^- coordination to Pd, and it elutes prior to $[Mo_3S_4(H_2O)_9]^{4+}$. Elution is also possible with 2 M Hpts, and in this case the behaviour is typical of 4+ charge, consistent with the existence of a water molecule at the Pd coordination site, i.e. $[Mo_3PdS_4(H_2O)_{10}]^{4+}$.

A similar behaviour is observed for the green $[Mo_3NiS_4(H_2O)_{10}]^{4+}$ cluster (UV-Vis band at 677 nm (ε = 610 $M^{-1}cm^{-1}$)), which was prepared by reacting Ni metal with $[Mo_3S_4(H_2O)_9]^{4+}$ at 90 º for 2 days.[20]

Kinetic and NMR experiments

Solutions of $[Mo_3PdS_4(H_2O)_{10}]^{4+}$ and $[Mo_3NiS_4(H_2O)_{10}]^{4+}$ were stored at low temperature under N_2 to avoid reaction with O_2. Standard Schlenck and manifold procedures were used to maintain an N_2 atmosphere during the preparation of the solutions and the kinetic runs. The kinetic experiments were carried out with a Cary 50 Bio UV-Vis spectrophotometer by mixing stock solutions of $[Mo_3PdS_4(H_2O)_{10}]^{4+}$ or $[Mo_3NiS_4(H_2O)_{10}]^{4+}$ and H_3PO_2. The experiments were carried out at 25.0 ± 0.1 ºC under pseudo first order conditions of H_3PO_2 excess, with the ionic strength adjusted to I = 2.00 ± 0.01 M with Hpts/Lipts mixtures. The complex solutions were prepared at concentrations of $(2.0\text{-}2.4)\times10^{-3}$ M in Hpts 2.0 M, and preliminary experiments at two different complex concentrations were carried out to confirm the first-order dependence of the observed rate constants on the complex concentration. The complex concentration was estimated from the UV-Vis spectra and the Hpts concentration was determined by titration with KOH (Phenolphthalein indicator). Stock H_3PO_2 solutions were prepared in water and titrated with KOH (Phenolphthalein indicator). These stock solutions were then mixed with Hpts/Lipts solutions whose acidity was also determined by KOH titration. A similar procedure was used for the experiments with H_3PO_4.

The reaction kinetics were monitored by recording the spectral changes with time and analysing the data with the SPECFIT.[29] The analysis required the use of a two-step kinetic model and provided the rate constants for each step as well as the calculated spectra for reagents, intermediate and reaction products. Reported rate constants are the average of at least three separate experiments.

The NMR experiments were carried out with a Varian Unity 400 spectrometer using the standard pulse sequences provided by the manufacturer. The chemical shifts in the ^{31}P NMR

spectra are reported with respect to external H_3PO_4. The samples were prepared under an inert atmosphere of N_2 by adding different aliquots of a H_3PO_2 solution to an NMR tube containing a solution of the starting complex.

Computational Details

All calculations were performed using the GAUSSIAN 03 series of programs[30] together with B3LYP functional.[31, 32] Two kinds of basis set systems were used. In the geometry optimization, the basis set system used (BS-I) was the double-ξ pseudo-orbital basis set LanL2DZ, in which the inner electrons of Mo, Pd and P atoms are represented by the relativistic core LanL2 potential of Los Alamos,[30, 33] and its associated double-ξ basis set for the outer ones. In the case of the P atoms, polarization and diffuse functions were added to the standard basis functions.[34] All other atoms were described with the double-ξ D95v basis set.[35] All geometry optimizations were performed without any symmetry constrains and for compounds that have multiple conformations, efforts were made to find the lowest energy conformation by comparing the structures optimized from different starting geometries. The nature of each stationary point was checked by diagonalizing the Hessian matrix to determine the number of imaginary frequencies (zero for the local minima and one for the TSs). The intrinsic reaction coordinate (IRC)[36] pathways from the TSs down to the two lower energy structures have been traced using the second-order González-Schelegel integration method[37, 38] in order to verify that each saddle point links the two putative minima. In the cases in which transition states could not be located, relaxed scans has been performed using in each case as reaction coordinate the most appropriate distance.

Solvent effects were taken into account by means of polarised continuum model (PCM)[39, 40] calculations using standard options.[30] The reported energies are given in aqueous solution (ε = 78.39) and were computed by single-point calculations with a better basis set system (BS-II), using the geometries optimized in the gas phase by the B3LYP/BS-I method. In BS-II, the same basis set and ECPs as those of BS-I were used for Mo and Pd atoms. The 6-311+G (3df,2p) basis set was used for P, O and H atoms.

Acknowledgements

Financial support by the Spanish D. G. C., the E.U. FEDER program, the Universitat Jaume I-Fundació Bancaixa (research projects CTQ2006-14909-C02-01, CTQ2005-09270-C02-02,

CTQ2006-15447-C02-01, and P1-1B2005-15), and the Junta de Andalucía (Group FQM-137) is gratefully acknowledged. A. G. A. also acknowledges a predoctoral grant from the Spanish Ministerio de Ciencia y Tecnología.

References

1. K. B. Dillon, F. Mathey and J. F. Nixon, *Phosphorus: The Carbon Copy*, Wiley, New York, 1998 and references therein.
2. F. Mathey, *Phosphorus-carbon heterocyclic chemistry: the rise of a new domain*, Elsevier, Oxford, 2001.
3. C. M. Nagaraja, M. Nethaji, and B. R. Jagirdar, *Inorg. Chem.*, 2005, **44**, 6203.
4. C. M. Nagaraja, P. Parameswaran, E. D. Jemmis, and B. R. Jagirdar, *J. Am. Chem. Soc.*, 2007, **129**, 5587.
5. F. A. Cotton, G. Wilkinson, C. A. Murillo and M. Bochmann, *Advanced Inorganic Chemistry*, 6th edn, John Wiley and Sons, New York, 1999, pp. 380-420.
6. N. N. Greenwood and A. Earnshaw, *Chemistry of the Elements*, Pergamon Press, Oxford, 1998, pp. 513-514.
7. A. Fratiello and E. W. Anderson, *J. Am. Chem. Soc.*, 1963, **85**, 519.
8. T. E. Haas and H. G. Gillmann, *Inorg. Chem.*, 1968, **7**, 2051.
9. J. W. Larson, *Polyhedron*, 1990, **9**, 1071.
10. J. R. Van Wazer, *Phosphorus and Its Compounds*, Interscience, New York, 1958, pp. 364-367.
11. D. N. Akbayeva, M. Di Vaira, S. S. Costantini, M. Peruzzini, and P. Stoppioni, *Dalton Trans.*, 2006, 389.
12. M. N. Sokolov, E. V. Chubarova, K. A. Kovalenko, I. V. Mironov, A. V. Virovets, E. V. Peresypkina, and V. P. Fedin, *Russ. Chem. Bull,* 2005, **54**, 615.
13. R. Hernandez-Molina, M. N. Sokolov, M. Clausen, and W. Clegg, *Inorg. Chem.*, 2006, **45**, 10567.
14. M. N. Sokolov, E. V. Chubarova, A. V. Virovets, R. Llusar, and V. P. Fedin, *J. Cluster Sci.*, 2003, **14**, 227.
15. M. N. Sokolov, R. Hernandez-Molina, W. Clegg, V. P. Fedin, and A. Mederos, *Chem. Commun.*, 2003, 140.
16. M. N. Sokolov, A. V. Virovets, D. N. Dybtsev, E. V. Chubarova, V. P. Fedin, and D. Fenske, *Inorg. Chem.*, 2001, **40**, 4816.
17. R. Hernández-Molina, I. Kalinina, M. N. Sokolov, M. Clausen, J. González Platas, C. Vicent, and R. Llusar, *Dalton Trans.*, 2007, **5**, 550.
18. A. G. Algarra, M. G. Basallote, M. J. Fernandez-Trujillo, R. Hernandez-Molina, and V. S. Safont, *Chem. Commun.*, 2007, **29**, 3071.
19. D. M. Saysell, G. J. Lamprecht, J. Darkwa, and A. G. Sykes, *Inorg. Chem.*, 1996, **35**, 5531.
20. D. M. Saysell, C. D. Borman, K. C. D., and A. G. Sykes, *Inorg. Chem.*, 1996, **35**, 173.
21. A. V. Prisyazhnyuk and Y. V. Babin, *J. Struct. Chem.*, 2005, **46**, 164.
22. E. M. Georgiev, J. Kaneti, K. Troev, and D. M. Roundhill, *J. Am. Chem. Soc.*, 1993, **115**, 10964.
23. R. Hernandez-Molina, M. N. Sokolov, and A. G. Sykes, *Acc.Chem. Res.*, 2001, **34**, 223.

24. R. Hernandez-Molina and A. G. Sykes, *J. Chem. Soc., Dalton Trans.*, 1999, 3137.
25. C. A. Routledge and A. G. Sykes, *J. Chem. Soc., Dalton Trans.*, 1992, 325.
26. M. N. Sokolov, N. Coichev, H. D. Moya, R. Hernandez-Molina, B. C. D., and A. G. Sykes, *J. Chem. Soc., Chem. Commun.*, 1997, **11**, 1863.
27. V. P. Fedin, M. N. Sokolov, A. V. Virovets, N. V. Podberezskaya, and V. E. Fedorov, *Inorg. Chim. Acta*, 1998, **269**, 292.
28. T. Murata, H. Gao, Y. Mizobe, F. Nakano, S. Motomura, T. Tanase, S. Yano, and M. Hidai, *J. Am. Chem. Soc.*, 1992, **114**, 8287.
29. R. A. Binstead, B. Jung and A. D. Zuberbühler, *SPECFIT/32*, Spectrum Software Associates, Chappel Hill, 2000.
30. Gaussian 03, Revision E.01, M. J. Frisch, G. W. Trucks, H. B. Schlegel, G. E. Scuseria, M. A. Robb, J. R. Cheeseman, J. A. Montgomery, Jr., T. Vreven, K. N. Kudin, J. C. Burant, J. M. Millam, S. S. Iyengar, J. Tomasi, V. Barone, B. Mennucci, M. Cossi, G. Scalmani, N. Rega, G. A. Petersson, H. Nakatsuji, M. Hada, M. Ehara, K. Toyota, R. Fukuda, J. Hasegawa, M. Ishida, T. Nakajima, Y. Honda, O. Kitao, H. Nakai, M. Klene, X. Li, J. E. Knox, H. P. Hratchian, J. B. Cross, V. Bakken, C. Adamo, J. Jaramillo, R. Gomperts, R. E. Stratmann, O. Yazyev, A. J. Austin, R. Cammi, C. Pomelli, J. W. Ochterski, P. Y. Ayala, K. Morokuma, G. A. Voth, P. Salvador, J. J. Dannenberg, V. G. Zakrzewski, S. Dapprich, A. D. Daniels, M. C. Strain, O. Farkas, D. K. Malick, A. D. Rabuck, K. Raghavachari, J. B. Foresman, J. V. Ortiz, Q. Cui, A. G. Baboul, S. Clifford, J. Cioslowski, B. B. Stefanov, G. Liu, A. Liashenko, P. Piskorz, I. Komaromi, R. L. Martin, D. J. Fox, T. Keith, M. A. Al-Laham, C. Y. Peng, A. Nanayakkara, M. Challacombe, P. M. W. Gill, B. Johnson, W. Chen, M. W. Wong, C. Gonzalez, and J. A. Pople, Gaussian, Inc., Wallingford CT, 2004.
31. A. D. Becke, *J. Phys. Chem.*, 1993, **98**, 5648.
32. C. T. Lee, W. T. Yang, and R. G. Parr, *Phys. Rev. B*, 1988, **37**, 785.
33. P. J. Hay and W. R. Wadt, *J. Chem. Phys.*, 1985, **82**, 299.
34. C. E. Check, T. O. Faust, J. M. Bailey, B. J. Wright, T. M. Gilbert, and L. S. Sunderlin, *J. Phys. Chem. A*, 2001, **105**, 8111.
35. T. H. Dunning, Jr. and P. J. Hay, *Modern Theoretical Chemistry*, ed. J. F. Schaefer, III, Plenum, New York, 1976, pp. 1-28.
36. K. Fukui, *J. Phys. Chem.*, 1970, **74**, 4161.
37. C. Gonzalez and H. B. Schlegel, *J. Phys. Chem.*, 1990, **94**, 5523.
38. C. Gonzalez and H. B. Schlegel, *J. Chem. Phys*, 1991, **95**, 5853.
39. M. Cossi, G. Scalmani, N. Rega, and V. Barone, *J. Chem. Phys.*, 2002, **117**, 43.
40. J. Tomasi, B. Mennucci, and R. Cammi, *Chem. Rev.*, 2005, **105**, 2999.